Anomalous low impedance for small platinum microelectrodes

Bo Fan[1], Jacob T. Robinson[1,2,3]

1. *Department of Electrical and Computer Engineering, Rice University, Houston, Texas 77005, United States*
2. *Department of Bioengineering, Rice University, Houston, Texas 77005, United States*
3. *Department of Neuroscience, Baylor College of Medicine, Houston, Texas 77030, United States*

Abstract

Electrical measurement of the activity of individual neurons is a primary goal for many invasive neural electrodes. Making these “single unit” measurements requires that we fabricate electrodes small enough so that only a few neurons contribute to the signal, but not so small that the impedance of the electrode creates overwhelming noise or signal attenuation. Thus, neural electrode design often must strike a balance between electrode size and electrode impedance, where the impedance is often assumed to scale linearly with electrode area. Here we test this assumption by measuring the impedance at 1 kHz for differently sized electrodes. Surprisingly, we find that for Pt electrodes (but not Au electrodes) this assumption breaks down for electrodes with diameters of less than 10 microns. For these small sizes, Pt electrodes have impedance values that are up to 3-fold lower than expected. By investigating the impedance spectrum of Pt and Au electrodes we find a transition between planar and spherical diffusion for small electrodes combined with the pseudo-capacitance of proton adsorption at the Pt surface can explain this anomalous low impedance. These results provide important intuition for designing small, single unit recording electrodes. Specifically, for materials that have a pseudo-capacitance or when diffusional capacitance dominates the total impedance, we should expect small electrodes will have lower-than-expected impedance values allowing us to scale these devices down further than previously thought before thermal noise or voltage division limits the ability to acquire high-quality single-unit recordings.

Introduction:

Neurons, as the fundamental functional units of the nervous network, communicate using electrophysiological signals[1]. This makes neural electrodes the most commonly used tools for numerous discoveries in neuroscience[2-5] and clinical therapies[6,7]. Penetrating microelectrodes can be implanted deep in the brain for extracellular recording from nearby neurons. Extracellular recordings are a mixture of local-field potential(LFP) and single-unit recording, which can be separated by filtering. The filtering bandwidth is 300-5000 Hz for single unit recording and < 300 Hz for LFP signals. Stable, chronic and high-quality single unit recording is essential to understand the neural networks on cellular levels[8,9], and it provides the most precise control in brain-machine interface applications[6,7].

Small electrodes are desirable for recording the activity of individual neurons (or “single units”) because their high spatial resolution allows them to record higher amplitude signals compared

to large electrodes[10]. In addition, for penetrating electrodes, smaller footprints reduce the damage to neural tissue upon implantation. On the other hand, smaller electrodes also have a higher impedance, which can reduce the quality of neural recordings. This high impedance can decrease the signal-to-noise ratio(SNR) in two ways. First, it leads to higher thermal noise, which increases as impedance increases[11,12]. Second, it creates a voltage divider, which consists of the electrode and the recording system in series[11-13]. As a result, higher impedance above 2-5 MΩ[11,13] can cause greater signal attenuation.

The important trade-offs in performance as a function of electrode size, makes it important to understand how the impedance scales with the electrode area, particularly for ultra-small electrodes. For planar electrodes it is typically assumed that impedance is inversely proportional to the electrode area[12,14] and thus electrode materials are typically characterized by a specific impedance (impedance times area) that is assumed to be a constant for that material. For volumetric conductors, like poly(3,4-ethylenedioxythiophene)(PEDOT) the impedance scales inversely with the volume of the electrode coating[15]. For planar metallic electrodes, a systematic study of impedance scaling in Pt, gold and PEDOT coated electrodes with radius ranging from 10 - 1000 um concluded that the porous coatings contribute to lower charge transfer resistance and better capacitive coupling of the electrode[16].

Recently we noted deviations from the linear relationship between impedance and electrode area when investigating planar and porous Pt electrodes which became pronounced for small feature sizes[12]. Here, we systematically study the impedance of Pt and Au electrodes as a function of size from diameters ranging from 3 - 125 µm to see if the impedance deviates from the expected linear relationship and what mechanism may explain this deviation.

Results:

To evaluate the scaling of electrode impedances we first fabricated raised Pt microelectrodes with radius ranging from 3 to 125 µm using standard microfabrication techniques[12] (see Methods). Briefly we fabricated 16-channel flexible microelectrodes using SU8 as an insulation layer. All 16 channels, though exposed electrodes are of different sizes, share one large via on the top SU8 for the raised structure(figure 1a).

We then measured the 1 kHz impedance and electrochemical impedance spectra (EIS) for each differently sized electrode(SI figure 1a,1d). For these measurements we used a Gamry 600+ with a three-electrode set up in 1X PBS solution. We used Ag/AgCl as the reference electrode and a bare Pt wire as the counter electrode.

When we plotted these 1 kHz impedance data versus radius on a log scale we were surprised to find that impedances deviated from a linear relationship for electrodes smaller than 10 µm (figure 2a). In larger electrodes(radius r >= 10 µm), the impedance has a dependence of $r^{-1.64}$. Interestingly, we found that the impedance of small electrodes with radius of 3 µm and 5 µm deviates from the linear fit of larger electrodes with radius greater than 10 µm. In this region, the impedance scales with a weaker dependence of the electrode radius ($r^{-0.83}$). We confirmed that

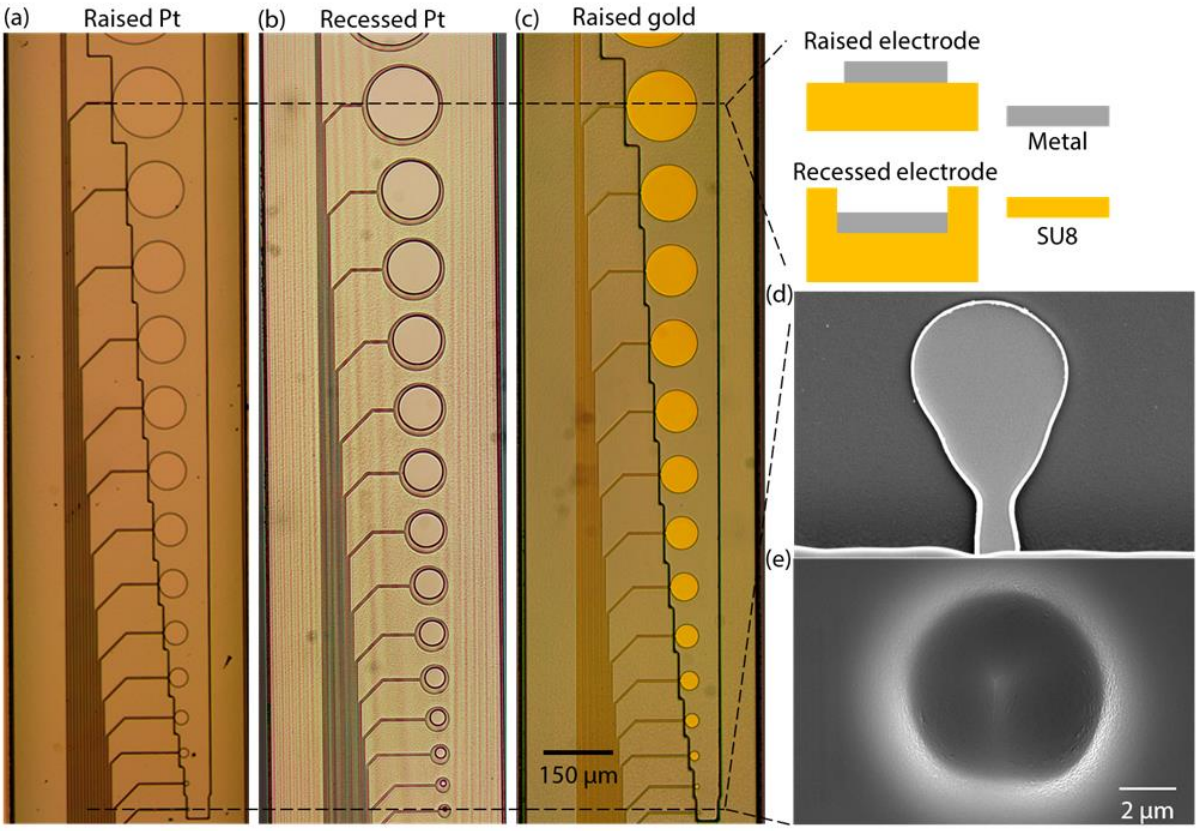

Figure 1. Microscopic image and SEM image of raised Pt, recessed Pt and raised Au electrodes. (a)-(c) 5X microscopic image of raised Pt, recessed Pt and raised Au electrodes, respectively. Inlet: Raised electrodes(Top) and recessed electrodes(Bottom). (d) SEM image of a raised Pt electrode with a radius of 3 µm. (e) SEM image of a recessed Pt electrode with a radius of 3 µm.

this deviation was not a fabrication error, by collecting SEM images of the smallest electrodes(figure 1d) and found that the electrode size is not significantly larger than designed.

We hypothesized that this deviation could be the result of the raised edges of the Pt electrode contributing to a larger electrode area, but recessed electrodes(figure 1b) also showed a similar anomalous low impedance. When we fabricated and tested electrodes with no exposed edges we also found the similar EIS(SI figure 1b, 1e) and 1 kHz impedance across all the sizes(figure 2b). Linear fits to these data showed nearly identical scaling with for large electrodes(>= 10 µm) as we had seen in the raised Pt electrode case ($r^{-1.64}$). Smaller electrodes also showed a reduced dependence on radius, but not as significant reduction as we observed for small raised Pt electrodes ($r^{-1.17}$).

By examining the resistance and reactance from our EIS data we determined that the deviation at small electrode sizes originates from the electrode capacitance (figure 2g, 2h). This can be seen by the fact that other than the two largest electrodes with radius of 100 and 125 µm, where

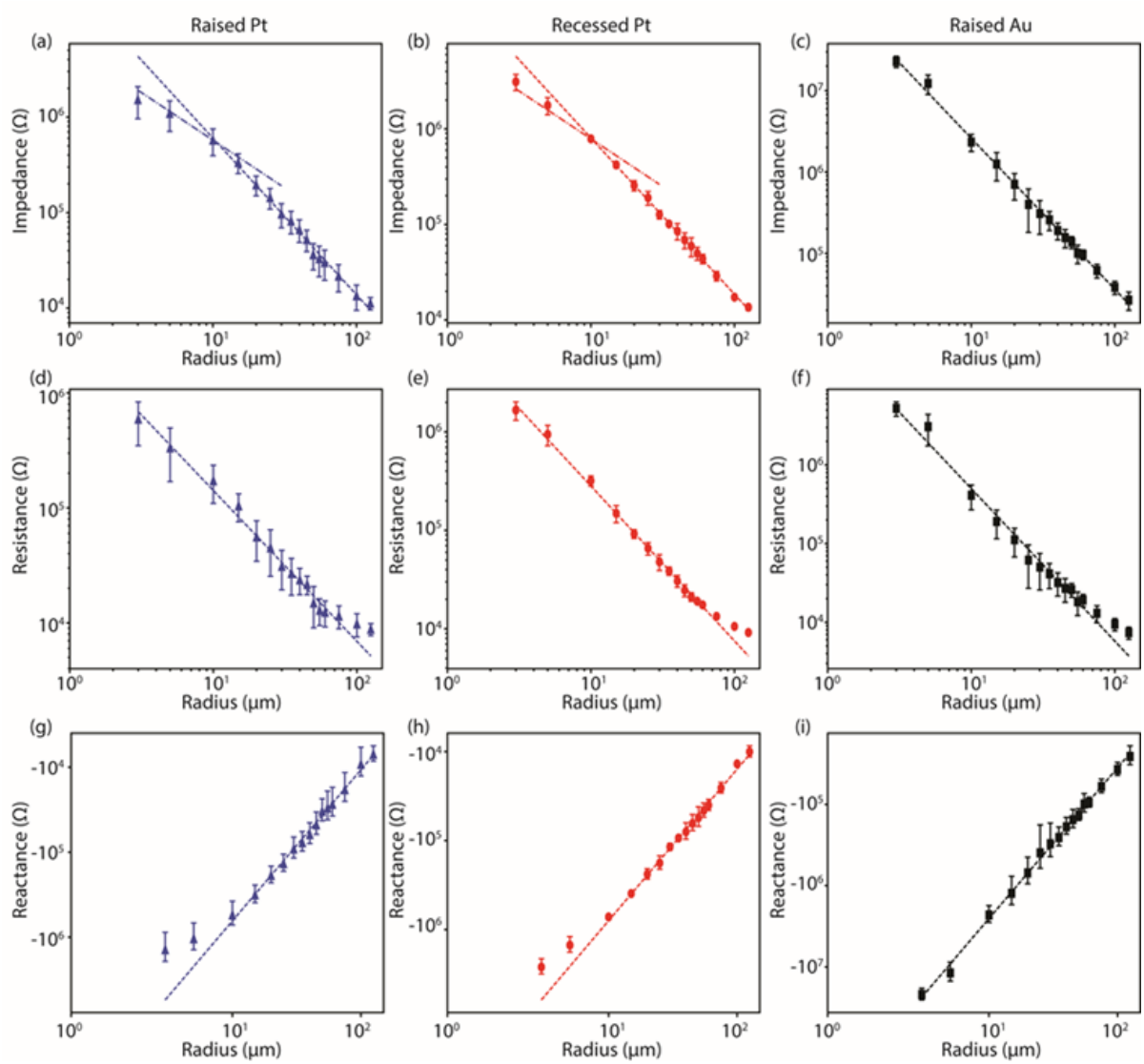

Figure 2. Impedance, resistance and reactance at 1 kHz of raised Pt, recessed Pt and raised Au electrodes. (a) Corrected impedance of raised Pt electrodes at 1 kHz in log scale, slope of linear fit for larger electrodes is -1.64(dash line), a guideline with a slope of -1 is also shown(dot-dash line). (b) Corrected impedance of recessed Pt electrodes at 1 kHz in log scale, slope of linear fit for larger electrodes is -1.64(dash line), a guideline with a slope of -1 is also shown(dot-dash line). (c) Corrected impedance of raised Au electrodes at 1 kHz in log scale, slope of linear fit for all electrodes is -1.86(dash line). (d) Corrected resistance of raised Pt electrodes at 1 kHz in log scale, slope of linear fit for larger electrodes is -1.31(dash line). (e) Corrected resistance of recessed Pt electrodes at 1 kHz in log scale, slope of linear fit for larger electrodes is -1.57(dash line). (f) Corrected resistance of raised Au electrodes at 1 kHz in log scale, slope of linear fit for all electrodes is -1.94(dash line).(g) Corrected reactance of raised Pt electrodes at 1 kHz in log scale, slope of linear fit for larger electrodes is -1.78(dash line). (h) Corrected reactance of recessed Pt electrodes at 1 kHz in log scale, slope of linear fit for larger electrodes is -1.70(dash line). (i) Corrected reactance of raised Au electrodes at 1 kHz in log scale, slope of linear fit for all electrodes is -1.86(dash line).

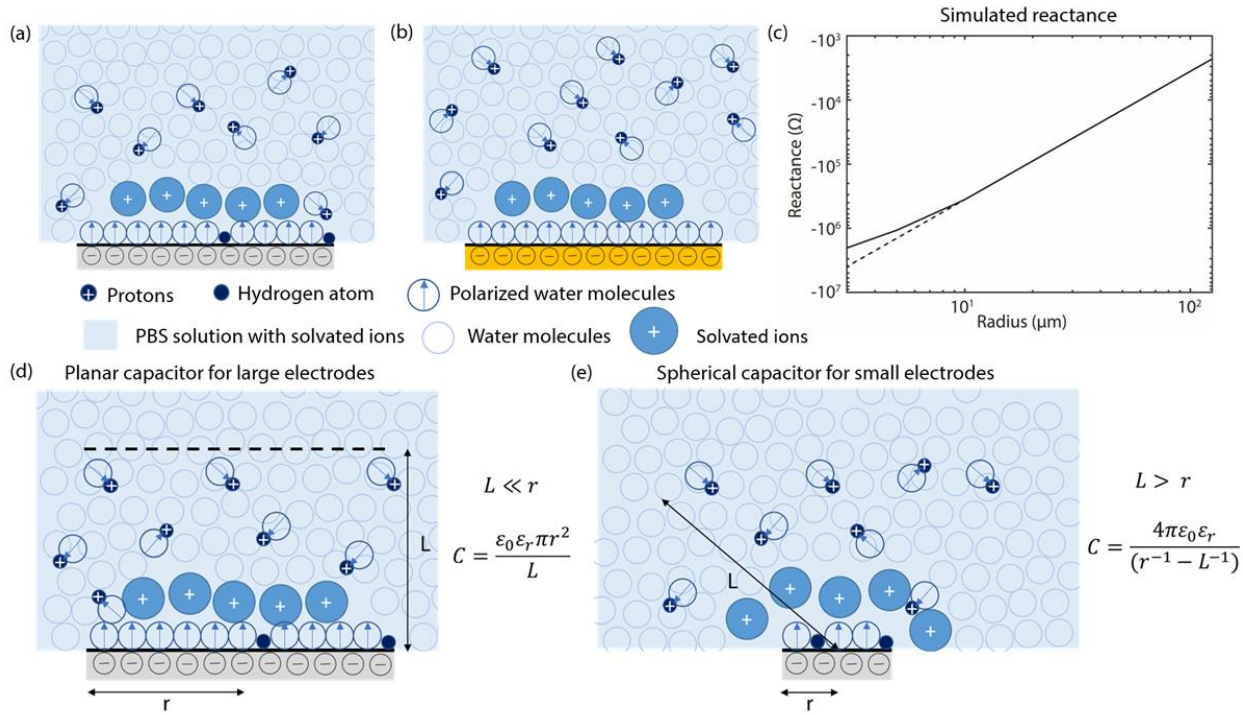

Figure 3. Equivalent circuit and diffusion model of Pt and Au electrodes. (a)Pseudo-capacitance(H atom adsorption) and double layer capacitance(polarized water molecules) of Pt electrodes, the other solvated ions are not shown. (b) Double layer capacitance(polarized water molecules) of Au electrodes, the other solvated ions are not shown. (c) Simulated reactance of Pt electrodes using the equation of planar capacitor for large electrodes(>= 10 μm) and that of spherical capacitor for small electrodes, as shown in (d) and (e). The thickness of the capacitive layer is assumed to be 20 μm. (e) For large electrodes, of which the thickness of the capacitive layer is less than the radius of the electrode, the boundary of the capacitive layer is parallel to the electrode surface and forms a planar capacitor with an area dependence of r^{-2}. (f) For small electrodes(r < 10 μm), the thickness of the capacitive layer is greater than the radius, the boundary of the capacitive layer is a half sphere, this half sphere capacitor is dependent on r^{-1}.

series resistance dominates the total impedance[16], the resistance fell on a linear fit for all electrode sizes, even for electrodes smaller than 10 μm ($r^{-1.31}$ for raised Pt electrodes and $r^{-1.57}$ for recessed Pt electrodes). On the other hand, the reactance shows a similar deviation in small electrodes as observed for total impedance: for larger electrodes, the reactance is dependent on $r^{-1.78}$ for raised Pt electrodes and $r^{-1.70}$ for recessed Pt electrodes.

Based on these data we hypothesized that this deviation in capacitance is caused by pseudo-capacitance related to hydrogen atom adsorption on the Pt electrode. We then tested this hypothesis by comparing impedance measurements to Au electrodes that do not adsorb hydrogen atoms. For these experiments we fabricated raised gold electrodes of the same design as raised Pt electrodes(figure 1c). From the EIS measurement, we noticed that the impedance of small gold electrodes is in the range of 10 MΩ, which is comparable to the shunt

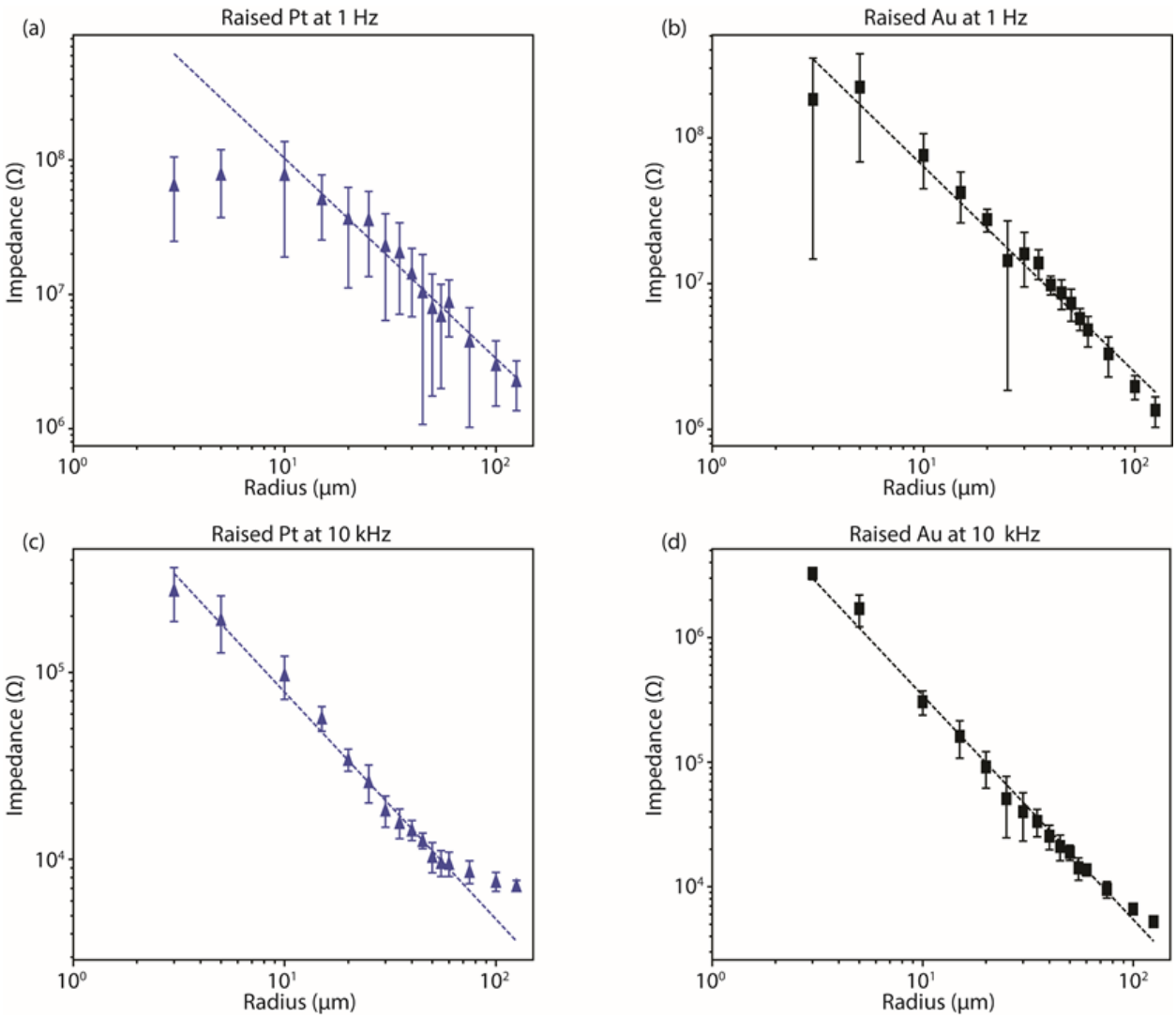

Figure 4. Impedance of raised Pt and raised Au electrodes at 1 Hz and 10 kHz. (a) Impedance of raised Pt electrodes at 1 Hz showing that for large electrodes with radius greater than 10 μm, the impedance scales with the dashed line ($r^{-1.49}$) , while for small electrodes, the impedance is dominated by reactance and is almost not related to the radius of electrodes. (b) Impedance of raised Au electrodes at 1 Hz scale as $r^{-1.41}$ (dashed line) for electrodes of all sizes. (c) Impedance of raised Pt electrodes at 10 kHz scales as $r^{-1.21}$ (dashed line) for electrodes of all sizes. (d) Impedance of raised Au electrodes at 10 kHz scales as $r^{-1.80}$ (dashed line) for electrodes of all sizes.

capacitance of the system. We measured a shunt impedance of 30.73 MΩ at 1 kHz(SI figure 2). This shunt impedance is in parallel with the electrodes, so we corrected the measured EIS data with this value using Ohm's Law. The corrected impedance of raised gold electrodes at 1 kHz is shown in figure 2c, where the impedance has a dependence of $r^{-1.86}$ for all the sizes without any deviation.

A possible explanation for our observations is that when the electrode is large, a capacitive layer of hydrated protons in the solution forms a plane that is parallel to the electrode surface(figure 3d). As the electrode size becomes smaller than the thickness of this capacitive layer, then this layer acts as a spherical capacitor rather than a planar capacitor, and the scaling of the capacitances changes from r^{-2} to r^{-1}. This transition closely matches our observed scaling for Pt electrodes that transitions from $r^{-1.6}$ to $r^{-0.8}$ for raised electrodes and $r^{-1.6}$ to $r^{-1.2}$ for recessed electrodes. The deviation from r^{-2} to $r^{-1.6}$ is probably caused by surface roughness[17] and non-uniform distribution of the surface R-Cs[18,19], which are the most used explanations for constant phase elements. The spherical diffusion hypothesis is further supported by difference between raised and recessed Pt in the anomalous impedance regime. Raised Pt shows a larger effect ($r^{-0.8}$) than recessed Pt ($r^{-1.2}$), which is consistent with the spherical diffusion hypothesis because the 4 µm high SU8 sidewalls of the recessed electrodes break the integrity of the diffusion sphere and limit horizontal diffusion.

To confirm that the anomalous low impedance is capacitive in nature we plot the impedance as a function of electrode size at frequencies of 1 Hz and 10 kHz. As expected, we find that at 10 kHz the impedance of Pt electrodes looks similar to Au electrodes and shows no deviation from the log-linear fit ($r^{-1.6}$) (figure 4c, 4d). At 1 Hz, however, there is increased anomalous low impedance where electrodes with a radius of 10 µm begin to deviate from the log-linear fit for Pt, but we see no deviation for Au electrodes (figure 4a, 4b).These data are consistent with the hypothesis that diffusional capacitance is the source for the anomalous low impedance because at high frequencies we expect that diffusional capacitance will not dominate the impedance because the impedance is inversely proportional to frequency.

Discussion:

From our measurements we have found that for large Pt electrodes(r >= 10 µm) the impedance scales roughly with the electrode area (r^{-2}) as previously reported[16]; however, as the electrodes fall below 10 µm radius their 1 kHz impedance deviates from this linear relationship, transitioning from approximately a r^{-2} scaling to an r^{-1} scaling. This change in scaling matches a transition from a planar to spherical capacitive layer. Similar deviations in impedance for smaller electrodes have been reported in PEDOT coated electrodes[20], but there was no explanation provided. By comparing Pt and Au electrodes, we confirmed that the deviation caused by this capacitive layer is related to the chemisorption of hydrogen atoms on the Pt surface and can be explained as a transition from planar to spherical capacitance when the electrode radius becomes small compared to the thickness of the diffusion layer. The thickness of this layer becomes larger at low frequencies, which is also seen in our measurement of the 1 Hz impedance. Another way to think about this deviation is to consider the capacitance as total charge that can be stored by the Pt microelectrode: C = Q/dV, where total charge Q is the charge per in the volume above the electrode and dV is the potential difference between the electrode surface and the boundary of the capacitive layer with a thickness L. The diffusion layer thickness depends on concentration of the electrolyte and temperature. The total charge Q within this capacitive layer depends on the volume of this capacitive layer. For large electrodes, this volume forms a cylinder($\pi r^2 L$), for smaller electrodes with L ~ r this volume becomes a

sphere that scales with r^{-1}, and for very small electrodes at low frequencies (L >> r), this volume forms a diffusion sphere($2/3\pi L^3$) that is independent of the electrode radius (r^0 dependence). As a result, as we measure how impedance scales based on electrode size and frequency we find a transition of radius dependence from r^{-2} to r^{-1} and eventually r^0. This capacitive diffusion layer is a similar concept to the diffusional pseudo-capacitance reported in PEDOT electrodes[21].

This explanation for impedance reduction in electrodes with diffusional pseudo-capacitance is especially important for neural recording in the brain, where diffusion is more significant. In this case, the spherical diffusional pseudo-capacitance may contribute more to the impedance reduction than in PBS solution. For ultra-small microelectrodes, we found that at a critical size of radius less than 10 µm, 1 kHz impedance of electrodes made by materials with pseudo-capacitance is weakly related to electrode size. For larger electrodes with pseudo-capacitance, spherical electrodes might have smaller impedance than planar electrodes of the same area.

These results provide a new explanation for why porous coatings can significantly reduce the impedance: in addition to larger effective areas, the surface texture allows protons to approach the surface from many angles acting like an array of small electrodes where spherical diffusion dominates their impedance characteristics. In addition, this diffusional pseudo-capacitance can also explain why fractal electrodes or waffle shaped electrodes showed reduced impedance compared to planar electrodes of a similar area[12].

An open question is how these anomalously low impedance measurements affect neural electrode performance in vivo. It has been argued that the common target of 100 kΩ impedance at 1 kHz is not necessarily an important metric for high quality neural recordings given modern high-impedance neural amplifiers[13]. Indeed, if the electrode impedance is below the input impedance of the amplifier one would not expect signal attenuation provided there was sufficiently small stray capacitance in the electrode insulation[11,13]. Where this low impedance may help the most is for extremely small electrodes where one would expect thermal noise to overwhelm the signal amplitude if not for the anomalous low impedance of Pt electrodes. It remains to be seen if ultra-small Pt electrodes can indeed perform well for chronic neural recordings; however, promising results have been obtained in vitro for nano-scale Pt electrodes giving some prospect for similar performance in future in vivo probes[22,23].

Methods:

Fabrication:

All the electrodes are fabricated using a similar method as previously reported[12]. We first sputtered a release layer of 70 nm Al on a Si wafer(University Wafer). Followed by photolithography to pattern the bottom SU8: spin coated SU8 2005(MicroChem) at 5000 rpm for 30 s, resulting in a 4 µm thick layer, then prebaked at 65 ^{0}C and 95 ^{0}C for 1 min and 4 min, respectively. After exposure, the wafer was post-baked again at 65 ^{0}C and 95 ^{0}C for 1 min and 4 min, respectively, then developed in SU8 developer for 2 min. Next, LOR 3A was spin-coated at 2000 rpm for 1 min, baked at 100 ^{0}C and 150 ^{0}C for 2 min and 10 min as lift-off sacrificial layer. Then S1818 was spin-coated at 4000 rpm for 1 min, baked at 115 ^{0}C for 1 min. After exposure,

the wafer was developed in MF321 for 2 min. Prior to sputtering metal traces, the surface was treated with oxygen plasma at 100 W for 1 min to enhance adhesion. A 100 nm thick Pt layer was sputtered and lifted off with acetone. For gold electrodes, 8 µm-thick Ti was sputtered as an adhesion layer. Next, top insulation SU8 was patterned using the same steps as bottom SU8. For recessed electrodes, a dry etch was applied using Reactive Ion Etcher(Oxford 180) to open up the top SU8 vias for small electrodes. Before releasing, the microelectrodes were hard baked at 180 ^{0}C for 1 hour. The microelectrodes were released using MF 321 for 8 hours.

Electrical connection and EIS measurement:
After releasing, the microelectrodes were collected and soaked in DI water for 24 hours. For EIS measurement, the electrodes were connected to break-out boards(OSH Park) using silver print(Silver Print II, GC Electronics). The EIS was performed with a three-electrodes set up using a Gamry 600 + electrochemical station. The reference electrode was a silver-silver chloride(Gamry Instrument) standard electrode, and the counter electrode was a bare Pt wire(uGems). The electrodes emerged in 1X phosphate buffered saline (PBS) (Fisher). The EIS was measured from 100 kHz to 1 Hz, with 30 points per decade. The input voltage was 10 mV in root-mean-square.

References

1.Hong, G., & Lieber, C. M. (2019). Novel electrode technologies for neural recordings. Nature Reviews Neuroscience, 20(6), 330-345.

2.Galvani, L. (1791). De viribus electricitatis in motu musculari. Commentarius. De Bonoiensi Scientiarum et Artium Intituo atque Academie Commentarii, 7, 363-418.

3.Hodgkin, A. L., & Huxley, A. F. (1939). Action potentials recorded from inside a nerve fibre. Nature, 144(3651), 710-711.

4.Hubel, D. H. (1957). Tungsten microelectrode for recording from single units. Science, 125(3247), 549-550.

5.Hubel, D. H., & Wiesel, T. N. (1962). Receptive fields, binocular interaction and functional architecture in the cat's visual cortex. The Journal of physiology, 160(1), 106.

6.Schwartz, A. B., Cui, X. T., Weber, D. J., & Moran, D. W. (2006). Brain-controlled interfaces: movement restoration with neural prosthetics. Neuron, 52(1), 205-220.

7.Aregueta-Robles, U. A., Woolley, A. J., Poole-Warren, L. A., Lovell, N. H., & Green, R. A. (2014). Organic electrode coatings for next-generation neural interfaces. Frontiers in neuroengineering, 7, 15.

8.Yuste, R. (2015). From the neuron doctrine to neural networks. Nature reviews neuroscience, 16(8), 487-497.

9.Harris, K. D., Quiroga, R. Q., Freeman, J., & Smith, S. L. (2016). Improving data quality in neuronal population recordings. Nature neuroscience, 19(9), 1165-1174.

10.Viswam, V., Obien, M. E. J., Franke, F., Frey, U., & Hierlemann, A. (2019). Optimal electrode size for multi-scale extracellular-potential recording from neuronal assemblies. Frontiers in neuroscience, 13, 385.

11.Ludwig, K. A., Langhals, N. B., Joseph, M. D., Richardson-Burns, S. M., Hendricks, J. L., & Kipke, D. R. (2011). Poly (3, 4-ethylenedioxythiophene)(PEDOT) polymer coatings facilitate smaller neural recording electrodes. Journal of neural engineering, 8(1), 014001.

12.Fan, B., Rodriguez, A. V., Vercosa, D. G., Kemere, C., & Robinson, J. T. (2020). Sputtered porous Pt for wafer-scale manufacture of low-impedance flexible microelectrodes. Journal of Neural Engineering, 17(3), 036029.

13.Neto, J. P., Baião, P., Lopes, G., Frazão, J., Nogueira, J., Fortunato, E., ... & Kampff, A. R. (2018). Does impedance matter when recording spikes with polytrodes?. Frontiers in neuroscience, 12, 715.

14.Park, S., Song, Y. J., Boo, H., & Chung, T. D. (2010). Nanoporous Pt microelectrode for neural stimulation and recording: in vitro characterization. The Journal of Physical Chemistry C, 114(19), 8721-8726.

15.Bianchi, M., Carli, S., Di Lauro, M., Prato, M., Murgia, M., Fadiga, L., & Biscarini, F. (2020). Scaling of capacitance of PEDOT: PSS: volume vs. area. Journal of Materials Chemistry C, 8(32), 11252-11262.

16.Ganji, M., Elthakeb, A. T., Tanaka, A., Gilja, V., Halgren, E., & Dayeh, S. A. (2017). Scaling effects on the electrochemical performance of poly (3, 4-ethylenedioxythiophene (PEDOT), Au, and Pt for electrocorticography recording. Advanced Functional Materials, 27(42), 1703018.

17.Rammelt, U., & Reinhard, G. (1990). On the applicability of a constant phase element (CPE) to the estimation of roughness of solid metal electrodes. Electrochimica Acta, 35(6), 1045-1049.

18.Jorcin, J. B., Orazem, M. E., Pébère, N., & Tribollet, B. (2006). CPE analysis by local electrochemical impedance spectroscopy. Electrochimica Acta, 51(8-9), 1473-1479.

19.Oldham, K. B. (2004). The RC time “constant” at a disk electrode. Electrochemistry Communications, 6(2), 210-214.

20.Koutsouras, D. A., Gkoupidenis, P., Stolz, C., Subramanian, V., Malliaras, G. G., & Martin, D. C. (2017). Impedance Spectroscopy of Spin-Cast and Electrochemically Deposited PEDOT: PSS Films on Microfabricated Electrodes with Various Areas. ChemElectroChem, 4(9), 2321-2327.

21.Bobacka, J., Lewenstam, A., & Ivaska, A. (2000). Electrochemical impedance spectroscopy of oxidized poly (3, 4-ethylenedioxythiophene) film electrodes in aqueous solutions. Journal of Electroanalytical Chemistry, 489(1-2), 17-27.

22.Robinson, J. T., Jorgolli, M., & Park, H. (2013). Nanowire electrodes for high-density stimulation and measurement of neural circuits. Frontiers in neural circuits, 7, 38.

23.Xie, C., Hanson, L., Xie, W., Lin, Z., Cui, B., & Cui, Y. (2010). Noninvasive neuron pinning with nanopillar arrays. Nano letters, 10(10), 4020-4024.